Available online at www.sciencedirect.com
ScienceDirect
Journal of Nuclear Materials 363–365 (2007) 658–663
journal of nuclear materials
www.elsevier.com/locate/jnucmat

Scrape-off layer plasmas for ITER with 2nd *X*-point and convective transport effects

T.D. Rognlien [a,*], R.H. Bulmer [a], M.E. Rensink [a], J.N. Brooks [b]

[a] *Lawrence Livermore National Laboratory, P.O. Box 808, L-630, 7000 East Ave, Livermore, CA 94551, USA*
[b] *Argonne National Laboratory, Argonne, IL 60439, USA*

Abstract

Plasma fluxes to the divertor region in ITER near the magnetic separatrix have been modeled extensively in the past. The smaller, but potentially very important fluxes to the main chamber and outer divertor regions are the focus of the present paper. Two main additions to the usual transport modeling are investigated: namely, convective radial transport from intermittent, rapidly propagating 'blob' events, and inclusion of the magnetic flux-surface region beyond the second *X*-point that actually contacts the main-chamber wall. The two-dimensional fluid transport code UEDGE is use to model the plasma, while the energy spectrum of charge-exchange neutrals to the main chamber wall is calculated by the DEGAS 2 Monte Carlo code. Additionally, the spatial distribution of beryllium sputtered from the main chamber wall is determined in the fluid limit.
© 2007 Elsevier B.V. All rights reserved.

PACS: 52.40.Hf; 52.25.Fi; 52.55.Rk; 52.65.−y; 52.25.Vy

Keywords: Edge transport; Divertor modelling; Impurity transport; Non-diffusive transport, UEDGE

1. Introduction

Scrape-off layer (SOL) plasma characteristics are key in evaluating plasma fluxes to material surfaces that determine peak heat loads, material lifetime, and hydrogenic and impurity particle sources via recycling and sputtering. Because of the mixed-material aspect of the ITER main-chamber wall [1] (mostly beryllium (Be), with tungsten (W) just above the divertor and in the private-flux region) and the divertor plates (carbon (C)), it is important to model plasma fluxes to these specific areas and to determine the intermixing of materials owing to spatial transport and re-deposition of sputtering materials.

Two new aspects of divertor physics for ITER are analyzed in this paper: first, the effect of possible strong radial convection of SOL plasma to the main chamber wall and the resulting Be sputtering, and second, inclusion of the outer SOL corresponding to magnetic flux surfaces beyond the secondary *X*-point. The study thus provides an extension of the previous 2D plasma transport modeling where both effects were ignored, *e.g.*, Ref. [2]. Because the turbulent transport of hydrogen and impurities in the

* Corresponding author. Fax: +1 925 423 3484.
E-mail address: trognlien@llnl.gov (T.D. Rognlien).

0022-3115/$ - see front matter © 2007 Elsevier B.V. All rights reserved.
doi:10.1016/j.jnucmat.2007.01.128

outer SOL of ITER is not well characterized, the present analysis simply provides plausible estimates based on models used to explain experimental data from present-day devices, and thus gives a measure of the potential importance of the two new aspects. Rapid convective transport of plasma in the SOL has been observed or inferred by various diagnostics, such as Langmuir probes, gas-puff imaging and imaging of background H_α light ([3–5] and references therein). A theoretical description explains the strong convection as from polarization of plasma density 'blobs' owing to charge-separation from opposite ion and electron ∇B drifts, and the resulting $E \times B$ drift [6]. Analysis of data from Alcator C-Mod and DIII-D tokamaks indicate that the time-averaged radial convective velocity can reach 100 m/s or more, and appears to increase with edge density [5]. Likewise, coupled turbulence/transport simulations show time-averaged velocities in this range for DIII-D parameters [7]. The ubiquitous nature of such convection and just how it depends on operating modes is not well understood, but the effect seems stronger at higher densities approaching the Greenwald limit, which is where ITER will operate. In both experiments and simulations, the time-averaged radial velocity is much less than the peak radial velocity owing to the strongly intermittent nature of the turbulence. The impact of convective SOL edge-plasma transport has been analyzed previously for other devices [8,9].

As designed, there can be some significant radial distance between the ITER wall and the secondary separatrix determined by the magnetic flux-surface intersecting the second magnetic X-point at the top of ITER (see Fig. 1). The hydrogenic plasma striking the separate Be and W portions of the wall will be in this outer SOL region. The 2D UEDGE transport code [10] now includes the ability to simulate extended SOL plasmas including both the region between the primary and secondary separatrices, and the radial domain outside the secondary separatrix, which is referred to as the far SOL. The charge-exchange neutral hydrogen flux to the wall is assessed with the DEGAS 2 Monte Carlo neutral code [11]. The impurity level in the edge plasma and the spatially dependent redeposition fluxes of different impurities are modeled by the UEDGE multi-component fluid model; here, only Be physical sputtering and transport is considered. The sensitivity of the Be transport and profiles to different convective transport models for each impurity charge state is shown.

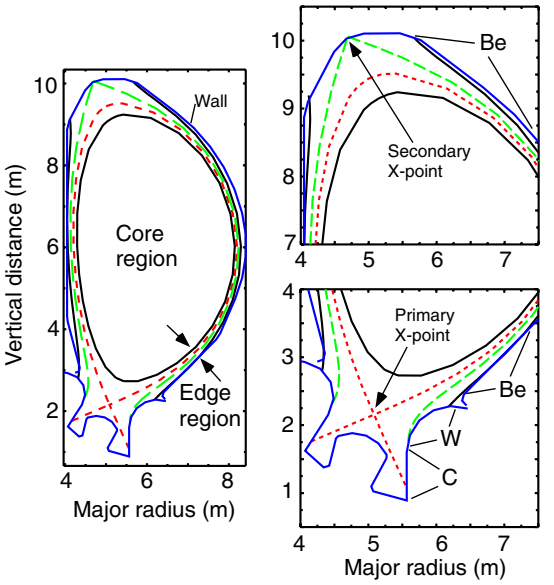

Fig. 1. ITER geometry showing various magnetic flux surfaces and outer wall, with blow-ups of top secondary X-point region and lower primary X-point. Two magnetic separatrices are primary (short dashed line (red), $\psi = 1.0$) and secondary (long-dashed line (green), $\psi = 1.035$). Extended SOL between secondary separatrix and solid line (black, $\psi = 1.09$). (For interpretation of the references to colour in this figure legend, the reader is referred to the web version of this article.)

The paper is organized as follows: the geometry and simulation models are given in Section 2, the hydrogenic plasma results are presented in Section 3, the Be sputtering and transport results are shown in Section 4, and a summary is presented in Section 5.

2. Geometry and simulation models

The ITER geometry used is shown in Fig. 1, where the interior lines all correspond to poloidal magnetic flux surfaces taken from the MHD equilibrium for ITER midway through its discharge. The dotted (red) line shows the primary separatrix adjacent to the core region, and the dashed (green) line is the secondary separatrix associated with the radially more distant X-point at the top of the device. The poloidal flux is $\psi = 1$ on the primary separatrix and $\psi = 1.035$ on the secondary separatrix; the extended SOL region considered here has $\psi_{max} = 1.09$. Previous transport modeling of ITER has taken the main chamber wall to be slightly inside the secondary separatrix to allow single-null simulations. However, as can be seen in Fig. 1, a substantial radial region (far SOL) exists between

the secondary separatrix and the actual ITER wall. Our extended simulations include the region out to the solid line just inside the outer wall, and thus directly encompass the lower tungsten (W) baffle noted in Fig. 1 and a portion of the upper Be wall where magnetic B-field lines intersect the wall.

The model for the edge plasma is taken from the strongly magnetized fluid equations of Braginskii [12] with some reductions as described in Ref. [10]. The 2D mesh is based on the magnetic flux surfaces. UEDGE [10] evolves moment equations for the plasma and neutral densities ($n_{i,n}$), parallel ion and neutral fluid momenta ($mn_{i,n}v_{\|i,n}$), and separate electron and ion energy densities ($3n_{e,i}T_{e,i}/2$). Here the electrostatic potential (ϕ) comes from the inertialess parallel electron momentum equation. For the simulations, the radial plasma particle flux is assumed of the form

$$\Gamma = -D\nabla_r n + V_c n, \tag{1}$$

where D and V_c are specified functions of distance normal (radial) to the magnetic flux-surface, and ∇_r is the normal derivative. For $mn_iv_\|$, n_eT_e and n_iT_i fluxes, additional diffusion coefficients are specified and these quantities are also transported by the particle flux [10]. Classical cross-field drifts are ignored here.

For self-consistent transport simulations, the hydrogenic and Be neutrals are described by a flux-limit fluid model, which gives reasonable neutral source profiles when compared to DEGAS 2 modeling. However to evaluate the detailed energy spectrum of the charge-exchange neutrals incident on the wall, DEGAS 2 [11] is used in a post-processing mode.

3. Results for the hydrogenic edge plasma

The base-case for ITER used here has 100 MW injected from the core into the edge region, split equally between ions and electrons. The hydrogenic deuterium/tritium components are treated as a single species with mass 2.5 AMU and a density of 6×10^{19} m^{-3} on the UEDGE core boundary. The anomalous radial diffusion coefficients at $D = 0.3$ m^2/s for density and $\chi_{e,i} = 1$ m^2/s for T_e, and T_i, as well as perpendicular viscosity for $v_\|$. A simplified fixed-fraction carbon impurity model is used with 3% carbon in coronal equilibrium; multi-species carbon produces similar results. The divertor and wall recycling coefficients are set to unity. For the standard edge domain treating only the single-null portion of the edge, the outer divertor peak particle power flux is 5 MW/m^2, and the peak radiation flux of 7 MW/m^2 due largely to carbon. These results are similar to the partially-detached operating mode of ITER [2].

To model the time-average of the strong 'blob' transport, a nearly exponentially increasing V_c is taken for the convective component of the radial fluid velocity, *i.e.*,

$$V_c(r) = V_1 \exp[(r - r_x)/r_w] + C_1, \tag{2}$$

with a maximum of about 70 m/s at the outer flux-surface, here corresponding to $\psi_{\max} = 1.034$ where r_x is the associated radial distance to the separatrix (having $r = 0$), $r_w = 0.027$ m, $V_1 = 70$ m/s and $C_1 = -1.4$ m/s. To model the ballooning nature of the turbulence, the convection is only applied to the outer half of the torus between the upper and lower X-points, except with $V_c = 0$ for the 0.5 m poloidal regions closest to the X-points. The magnitude and profile of V_c are in the range deduced from C-Mod and DIII-D data [5] and simulations of DIII-D edge turbulence [7].

The base-case ITER simulation is repeated with the addition of V_c, and the results are shown in Figs. 2 and 3. In Fig. 2(a), the radial ion velocity at the midplane is separated into convective and diffusive ($V_D = -D\nabla_r n_i/n_i$) components. For the base-case with $V_c = 0$, V_D is similar in the core, and rises to about 20 m/s half-way into the SOL before decreas-

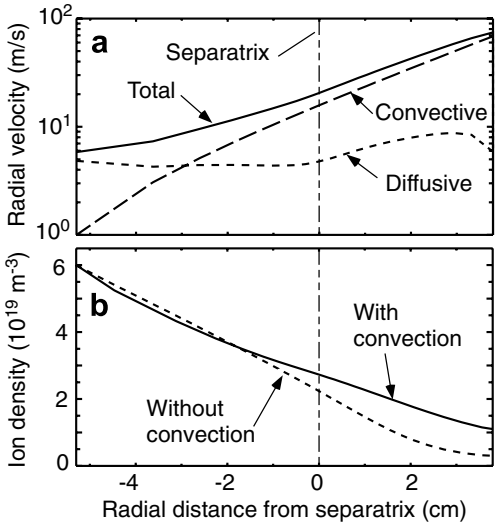

Fig. 2. Plasma radial velocity components are shown in (a) for the convective case (V_c from Eq. (2)), and in (b), the ion density with finite V_c and $V_c = 0$, both at the outer midplane.

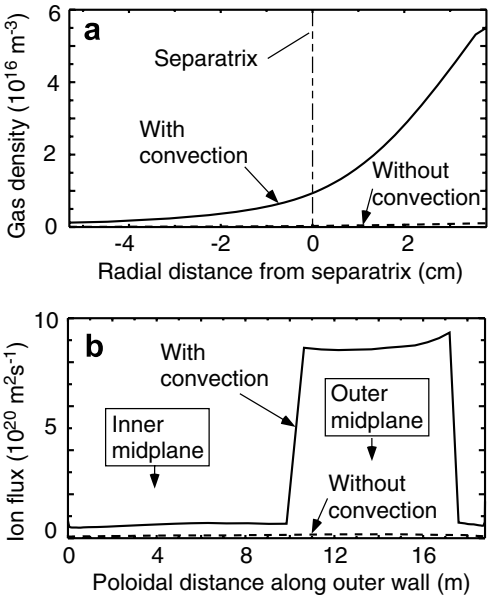

Fig. 3. In (a), neutral density at the outer midplane with and without V_c, and in (b), radial ion flux at the wall ($\psi_{max} = 1.035$) versus poloidal distance moving clockwise from the inner divertor.

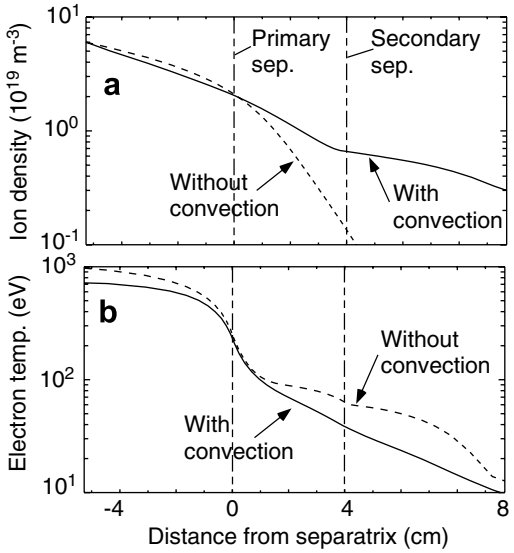

Fig. 4. Ion density for radially extended domain ($\psi_{max} = 1.09$) in (a), with and without V_c activated, and (b), the corresponding electron temperature.

ing to the wall. The ion density profiles are shown in Fig. 2(b) comparing the base- and finite-V_c cases. The largest difference is the higher SOL density with V_c, which is in turn largely the result of wall recycling producing a strong ionization source in the SOL. Fig. 3(a) shows the associated large increase in the neutral density when V_c is present. The increase in ion density, coupled with the large V_c at the wall, gives a large ion flux to the wall, shown in Fig. 3(b). This flux can give substantial sputtering of Be from the wall, as show in Section 4. With this specific choice for V_c, the total peak heat flux on the outer plate decreases from 12 to is 9.7 MW/m^2, while that to the inner plate increases somewhat.

Next, the region beyond the secondary separatrix, defined by the flux surface passing through the upper X-point in Fig. 1, is included in the simulation to $\psi_{max} = 1.09$. The wall region in the vicinity of the upper X-point behaves like another divertor with magnetic field-lines intersecting the wall, and the W baffle region in the lower divertor is included explicitly as an extended region of the lower divertor plate. The (constant) transport diffusion coefficients are the same as in other regions, and the convective velocity V_c, when activated, remains constant at its previous wall value of 68.6 m/s throughout the extended outer midplane region.

The resulting plasma density and electron temperature (T_e) are compared in Fig. 4 for the cases with V_c from Eq. (2) and that with $V_c = 0$. In both cases, the density near the second separatrix decreases about a factor of two from the $\psi_{max} = 1.035$ case owing to ions flowing into the far SOL region. Likewise the temperatures decrease by a factor of 1.5. In the far SOL, T_i is about twice T_e for finite V_c. The power flow across the secondary separatrix on the outside of the torus is 15 MW for finite V_c, and 6 MW for $V_c = 0$, compared to 100 MW injected across the core boundary. The particle flux reaching the new outer wall is reduced by a factor of 2–3 compared to the $\psi_{max} = 1.035$ case, with a large fraction of the difference flowing to the lower W baffle region that is assume not to sputtering owing to the low $(T_e, T_i) \sim (5,10)$ eV there. The peak heat flux on the outer divertor is about the same as the $\psi_{max} = 1.035$ case for the $V_c = 0$, but increases to $\sim$20 MW/m^2 for the finite V_c case owing to a large increase in T_e very near the primary strike point. Thus, the partially-detached solution can be sensitive to V_c (and also moderate changes in its profile).

4. Be sputtering and transport

One of the consequences of possible strong convective transport in the SOL of ITER is sputtering of wall material. We calculate the impact for the

finite V_c case using a multi-species Be simulation with UEDGE, where the sputtering produces a flux of Be neutrals from the main-chamber wall that are eventually ionized. Here Be is treated as a trace impurity with the hydrogenic plasma fixed at the profiles described in Section 3 for the finite V_c case and $\psi_{max} = 1.09$. The sputtered flux is taken from the incident hydrogen flux assuming an incident energy of $2T_i + 3T_e$, and is computed from a Be yield-curve. In addition to ion sputtering of Be, charge-exchange (CX) neutrals from recycled hydrogen can also sputter. The CX source is evaluated by DEGAS 2 [11] to obtain the full kinetic distribution. The procedure shows that the CX sputtering is a factor of 3–4 smaller than the ion sputtering and will make only a modest correction to the ion sputtering results.

The midplane Be density resulting from the main-chamber ion sputtering is shown Fig. 5(a) for two models of Be ion transport. The Be recycling coefficient is set to a small value (0.01) on all surfaces. The solid line has $V_c = 0$ for Be, and the chain-dot line assumes that low charge-states (on the periphery) are convected inwards and higher charges-states are convected outward with the hydrogen [8]; simple edge turbulence simulations show impurities being convected inward [9]. For the latter case, the convective velocities for charge-states (1, 2, 3, 4) are $(-V_c, -V_c/3, V_c/3, V_c)$. The largest difference between the two solutions is near the primary separatrix and the core, but even the $V_c = 0$ case has 0.33% Be in the core, which should be tolerable. Beryllium can also coat the carbon divertor plate and tungsten baffle, and the Be fluxes to those surfaces are shown in Fig. 5(b) for the Be diffusion-only case. Note that the Be flux is large near the inner strike point. The divertor flux for the variable-V_c Be case (not shown) is very similar, with a 30% reduction in the peak near the outer baffle. For the traditional ITER modeling case with $V_c = 0$, the ion and CX-neutral sputtering of Be are both smaller by orders of magnitude from the cases presented here.

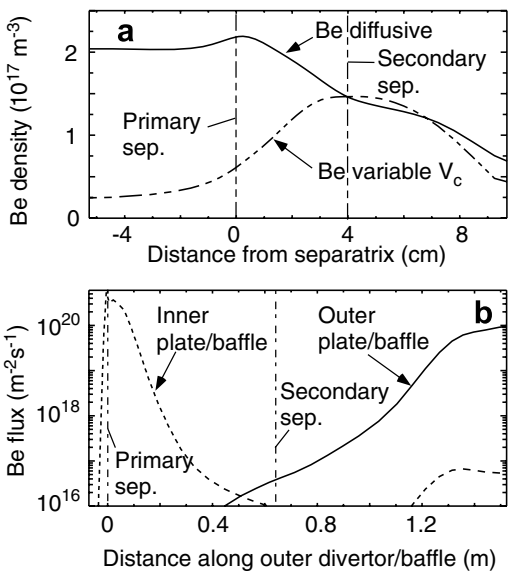

Fig. 5. In (a), midplane Be density for Be diffusion-only and Be variable convection cases, and (b), Be fluxes to the lower divertor for Be diffusion-only using the hydrogenic plasma shown in Fig. 4 with finite V_c. The inner divertor flux is plotted versus the outer plate coordinate to enable one to compare fluxes on the common flux surfaces between the primary and secondary separatrices.

5. Summary

The edge-plasma in ITER has been analyzed to assess two new effects: possible strong radial convective transport and the presence of the extended SOL outside the secondary separatrix. We find that these effects are potentially very important for predicting plasma-wall interactions in ITER. However, more detailed and systematic studies are required to draw final conclusions as various elements of the model are uncertain, especially the actual nature of the turbulent transport. This study has shown the following: (1), strong convective transport can result in significant sputtering of Be from the chamber walls, yielding concentration at the core boundary up to 0.67% and significant Be fluxes to the divertor regions; (2), inclusion of the secondary SOL reduces the hydrogen flux to the wall by ~1/3, partially diverting it to the baffle and 'upper divertor' region for this time-averaged model of convective transport (see next paragraph); and (3), the primary SOL and peak heat flux to the divertors can be sensitive to details of the V_c profile, even for the same overall peak magnitude.

Note that conclusion (2) just above may change when the time-dependent blob transport is included since the V_c used is a time-average value, whereas experiments and theory show that the peak V_c is much larger, but only occurs a small fraction of the time. This larger V_c should preferentially convect more plasma to the chamber wall before it can travel to the lower or upper divertors, and this is now being investigated with a time-dependent V_c in UEDGE.

Additionally, we are conducting 3D kinetic modeling of wall/divertor-sputtered impurity transport via the REDEP/WBC transport code package [13] for the UEDGE/DEGAS hydrogenic solutions. Kinetic effects can be especially important in the far SOL with weaker collisions. This modeling also uses a self-consistent mixed-material erosion/redeposition treatment for computing net erosion/growth for an 'all-metal' ITER boundary system, *e.g.*, a tungsten divertor with beryllium or tungsten coated first wall and computes tritium codeposition in redeposited beryllium. Initial results generally support the Be fluid modeling conclusions, showing very low wall erosion and acceptably low plasma contamination, for both Be and W walls. For the Be wall/W-divertor combination, the codes predict of order 1 nm/s Be growth over large portions of an initially-tungsten divertor for the convective regime, and zero net Be growth for the diffusion-only case. These initial WBC calculations use the narrower UEDGE plasma solution terminating at the secondary separatrix with an assumed plasma in the far SOL [14].

Acknowledgement

We thank S.I. Krasheninnikov for suggestions related to time-dependent 'blob' transport and D.P. Stotler for providing the DEGAS 2 code. This work was performed under the auspices of the US Department of Energy by the University of California Lawrence Livermore National Laboratory under contract No. W-7405-Eng-48.

References

[1] M. Shimada, A.E. Costly, G. Federici, et al., J. Nucl. Mater. 337–339 (2005) 808.
[2] A.S. Kukushkin, H.D. Pacher, D. Coster, et al., Nucl. Fus. 43 (2003) 716.
[3] B. LaBombard, M.V. Umansky, R.L. Boivin, et al., Nucl. Fus. 40 (2000) 2041.
[4] J.A. Boedo, D.L. Rudakov, R.A. Moyer, et al., Phys. Plasmas 10 (2003) 1670.
[5] B. Lipschultz, D. Whyte, B. LaBombard, Plasma Phys. Control. Fus. 47 (2005) 1559.
[6] S.I. Krasheninnikov, Phys. Lett. A 283 (2001) 368.
[7] T.D. Rognlien, M.V. Umansky, X.Q. Xu, et al., J. Nucl. Mater. 337–339 (2005) 327.
[8] A.Yu. Pigarov, S.I. Krasheninnikov, T.D. Rognlien, et al., Contribution Plasma Phys. 44 (2004) 228.
[9] M. Kotschenreuther, T.D. Rognlien, P. Valanju, Fus. Eng. Design 72 (2004) 169.
[10] T.D. Rognlien, D.D. Ryutov, N. Mattor, G.D. Porter, Phys. Plasmas 6 (1999) 1851.
[11] D.P. Stotler, C.F.F. Karney, et al., Contribution Plasma Phys. 40 (2000) 221, also <http://w3.pppl.gov/degas2/>.
[12] S.I. Braginskii, Transport processes in a plasma, in: M.A. Leontovich (Ed.), Reviews of Plasma Physics, vol. 1, Consultants Bureau, New York, 1965, p. 205.
[13] J.N. Brooks, Fus. Eng. Design 60 (2002) 515;
J.N. Brooks, Phys. Fluids 8 (1990) 1858.
[14] J.N. Brooks, J.P. Allain, T.D. Rognlien, Phys. Plasmas 13 (2006) 122502.